Contents lists available at ScienceDirect

Applied Catalysis B: Environmental

TiO2 Nanotube arrays: Influence of tube length on the photocatalytic degradation of Paraquat

Cédric B.D. Marien [a], Thomas Cottineau [a], Didier Robert [a,*], Patrick Drogui [b]

[a] Institut de Chimie et Procéídeís pour l'Energie, l'Environnement et la Santeí (ICPEES), CNRS-UMR7515-University of Strasbourg, Saint-Avold Antenna, Université de Lorraine, 12 rue Victor Demange, 57500 Saint-Avold, France
[b] Institut national de la recherche scientifique (INRS-Terre et Environnement), Université du Québec, 490 rue de la Couronne, Québec G1K 9A9, Canada

ARTICLE INFO

ABSTRACT

Highly ordered TiO2 nanotubes have attracted a lot of attention for the photocatalytic removal of organic pollutants. A few studies demonstrated that the tube morphology plays a key role on the photocatalytic activity. However, no studies have been performed to explain the optimal photocatalytic activity observed for a precise tube length. Here we studied how the morphology of the tubes evolves during anodic growth and we evaluated the corresponding photocatalytic activity. In our conditions, the optimal activity was found for 7 μm long tubes. The SEM study reveals that short tubes have a small pore opening thus hindering pollutant diffusion into the tubes. On the other hand, tubes longer than 7 μm have thinner walls due to etching by the fluoride ions. Consequently the volume of TiO2 decreases strongly in the upper part of the tubes as the tube length increase and light should travel a longer pathway before absorption and production of electron-hole pairs. Hence the organic species have to diffuse further and the photocatalytic activity decreases.

© 2016 Elsevier B.V. All rights reserved.

1. Introduction

Water contamination by organic pollutants has become a significant problem because these species are usually toxic and come from many different sources: herbicides, pesticides, pharmaceuticals and care products. Many organic compounds have an hydrophobic behavior thus are usually stored in the fat or in certain organs [1]. This induces a problem of bioaccumulation because these molecules are concentrated through the food chain. Consequently a great deal of attention must be paid to the removal of these organic compounds because their persistence in the environment is a major public health problem. On the other hand, it is estimated that 4 billion people have no or little access to clean water and millions of people die each year of water borne disease [2]. Consequently technological processes to remove these compounds are highly desired.

Removal of organic pollutants from water is a challenging issue. Current processes suffer from various drawbacks for example coagulation-flocculation or adsorption doesn't destroy the organic pollutants but simply transfers it from one phase to another. For chlorination, secondary products are expected to be toxic

(organochlorinated compounds) and could act as persistent organic pollutants [3]. Advanced oxidation processes are being explored for their ability to fully mineralize organic pollutants. These processes are based on the production of highly oxidizing species such as hydroxyl or superoxide radicals. Among these processes, photocatalysis is very promising because it is a non-selective process, the reactions occur at room temperature and the photocatalyst can be activated by solar irradiation.

Titanium dioxide (TiO2) is one of the most studied semiconductors due to its non-toxicity, high chemical stability (particularly to photocorrosion) and photocatalytic efficiency [4]. Photocatalytic removal of organic pollutants consists in illuminating a semiconductor, usually TiO2 with UV-light, to produce electron-hole pairs. After separation, the holes react with water or adsorbed OH^- and electrons react with dissolved dioxygen to produce respectively hydroxyl and superoxide radicals. These compounds are highly oxidizing species which react with the organic pollutants leading in some case to the complete mineralization. Here we studied the photocatalytic degradation of Paraquat (1,1-dimethyl-4,4-bipyridylium dichloride) a widely used herbicide which is known to be degraded by these oxidizing radicals [5,6]. The mechanism of photocatalytic degradation is known to produce monopyridone and dipyridone [7] and then after complete mineralization to CO$_2$, water, NH_4^+, NO_2^- and finally NO_3^- [8,9].
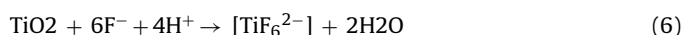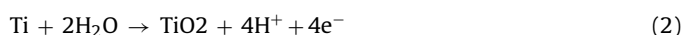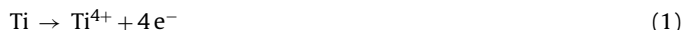
* Corresponding author.
E-mail address: didier.robert@univ-lorraine.fr (D. Robert).

Photocatalysis has been widely used with suspension of TiO_2 nanoparticles. However, the recovery of the catalyst involves expansive separation processes. The immobilization of TiO_2 on a substrate is attractive due to its simplicity of recovery. However for a same amount of TiO_2, a suspension offers a higher active surface area than a thin film due to the close packing in thin films. To overcome this problem, nanostructured thin films with high active surface area are desired for photocatalysis.

Controlling the porosity is usually performed thanks to the template-assisted method which involves a pore-directing agent to control the porosity: polystyrene spheres [10], polyethylene glycol [11] or anodic aluminium oxide [12]. However the removal of the template can lead to fragile thin films with poor mechanical stability. Moreover the template-assisted growth is time consuming and often involves several steps.

Electrochemical methods have been recently reported for the fabrication of various TiO_2 nanostructures: nanotubes [13], fishbone [14], mesosponge [15] or nanochannels [16]. The anodic growth consists in oxidizing a titanium foil in an adequate media to produce a porous TiO_2 coating on the surface. This approach is fast, facile and allows a precise control of the porosity. Moreover anodic TiO_2 nanostructures are produced on a conductive electrode which is ready-to-use for the photoelectrocatalytic removal of organic compounds [17]. Despite these advantages, only the tubular structure can be obtained at ambient temperature where a hot phosphate-glycerol electrolyte (temperature >150 °C) is required to produce other structures (fishbone, mesosponge and nanochannels). Consequently anodically grown TiO2 nanotubes have a great potential for photocatalysis due to their large internal surface area and their facile fabrication.

The anodic growth of TiO_2 nanotubes consists in applying a DC voltage on a Ti foil immersed in an organic electrolyte, usually ethylene glycol, with water and fluoride ions (third generation nanotubes) [18]. This growth can only be achieved under optimized conditions where equilibrium is reached between oxide formation (Eqs. (1)–(4)) and oxide dissolution (Eqs. (5) and (6)):

$$Ti \rightarrow Ti^{4+} + 4e^- \tag{1}$$

$$Ti + 2H_2O \rightarrow TiO2 + 4H^+ + 4e^- \tag{2}$$

$$Ti^{4+} + 4H2O \rightarrow Ti(OH)_4 + 4H^+ \tag{3}$$

$$Ti(OH)4 \rightarrow TiO_2 + 2H2O \tag{4}$$

$$Ti^{4+} + 6F^- \rightarrow [TiF_6{}^{2-}] \tag{5}$$

$$TiO2 + 6F^- + 4H^+ \rightarrow [TiF_6{}^{2-}] + 2H2O \tag{6}$$

The oxide dissolution produces a water soluble complex ($TiF_6{}^{2-}$). At the same time, hydrogen evolves at the counter electrode, usually platinum:

$$4H^+ + 4e^- \rightarrow 2H2 \tag{7}$$

The tube morphology has a significant influence on the photocatalytic performances of the TiO2 nanotubes for water depollution. Smith et al. [19] demonstrated that nanotubes with large diameters have a better photocatalytic activity because the photocatalyst surface is more available. Many reports also focus on the optimal tube length for photocatalytic degradation experiments: 6 µm [20], 16 µm [13], 17 µm [21] and 18 µm [22]. In these papers, the growth conditions are different thus the tube morphology (internal diameter and wall thickness) is expected to be different for a same tube length. Besides UV light is absorbed in the first 1–2 µm [23] thus the top morphology should play a key role. Mazzarolo et al. [24] investigated the influence of the top morphology on the photocatalytic activity. They revealed that tubes with a well defined open mouth have an enhanced photocatalytic activity compared to grassy tubes and tubes with an initiation layer. In this paper,
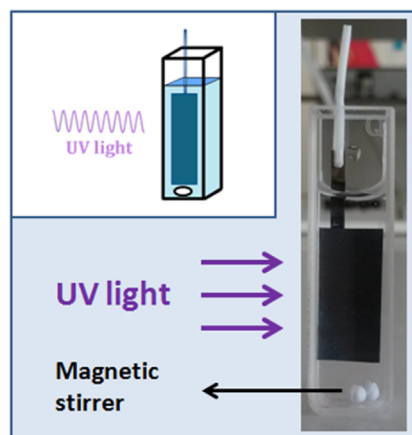
Scheme 1. Photocatalytic setup: quartz cuvette with a TiO_2/Ti sample and a small magnetic stirrer at the bottom.

we studied the influence of the top tube morphology for various lengths and we correlated this to the photocatalytic activity in the case of the degradation of Paraquat in water. The aim is to provide a basic understanding of the underlying mechanism.

2. Experimental methods

2.1. Electrochemical growth of TiO_2 nanotubes

Titanium foils (thickness: 125 µm) were purchased from Mateck (Germany). Samples were cut in 2×1.5 cm^2 pieces and welded on the backside with a thin titanium contact (0.4×2 cm^2). Surface impurities were removed by immersion in regia aqua (HCl/HNO$_3$-3/1 in volume) and then degreased by successive immersions, under ultrasonication in acetone, anhydrous ethanol and distilled water (5 min each). The samples were then dried with compressed air. Electrochemical anodisation was performed with a three-step process. First samples were preanodised at 60 V during 30 min at 20C° in ethylene glycol with NH4F (0.3 wt%) and H$_2$O (2 v%). The nanotube layer was then peeled-off by ultrasonication. The samples were then anodized in the same electrolyte with the same conditions during various durations. After anodisation, the samples were immediately transferred in a 5 wt% H3PO4 in ethylene glycol and immersed during 1 h. The post anodisation was then performed during 5 min at 60 V to produce an oxide layer that improves the nanotubes adhesion. Samples were finally immersed in ethanol during 1 h before calcination in air at 450 °C during 2 h (5 °C/min).

2.2. Samples characterization

SEM analysis were performed with a JEOL-JSM-7600F at the Coatings Research Institute (CoRI, Belgium). For thickness measurements, samples were wrapped in an epoxy resin. The surface of the epoxy was then polished to reveal the edge of the electrode perpendicular to the surface. Samples were platinized before analysis to avoid the charging effect. XRD allowed to examine the crystallinity thanks to a Shimadzu instrument (MiniFlex II) using the Cu k-alpha radiation.

2.3. Evaluation of the photocatalytic activity

Photocatalytic tests (Scheme 1) were performed with a quartz cuvette filled with 3 ml of Paraquat dichloride (10 ppm, Aldrich) at pH = 7 and a magnetic stirrer (3 mm). The concentration of Paraquat was followed at 257 nm thanks to Beer-Lambert law. Two UV lamps (8 W each) were used at 3 cm from the cuvette

and the irradiance was measured with a HD 9021 instrument from Delta Ohm: 13 W/m^2 (UV-A: 315–400 nm) and 50 mW/m^2 (UV-B: 280–315 nm). The samples were cut to fit in the cuvette (2 × 0.8 cm^2) and the exposed surface was precisely measured with the ImageJ software.

3. Results and discussion

3.1. Characterization of TiO$_2$-NT samples

Fig. 1 shows the tube morphology for various lengths. Short tubes (fig. 1A) represent the initiation layer with very small and disordered pores (thin channels). As the length increases, the pores and the channels are opening (fig. 1B and C). In our conditions, the opening is well-defined for 7 μm long tubes (fig. 1B). As the tube length increases the amount of TiO2 on the top is highly reduced due to chemical etching by the fluoride ions. These morphological features are expected to have a strong influence on the photocatalytic properties [24].

Fig. 1C shows very thin top tubes whereas they look thicker on Fig. 1D, because the 2D top view flattens the picture. Top views (Fig. 1) clearly demonstrate the wall thinning and the pore opening. Based on Scheme 2, we can estimate the pore size with the ImageJ software.

The wall thickness can be evaluated by dividing by 2 the distance between neighboring pores 2W. All the data are given in Table 1:

Table 1 allows to evaluate the amount of TiO$_2$ in the upper part of the tubes. Assuming straight tubes instead of the classical v-shape, we can calculate the volume V of TiO$_2$ in the tube wall with the following formula:

$$V = \pi L r_{ext}{}^2 - \pi L r_{int}{}^2$$

Since the external diameter is constant (2 $r_{ext} = 2W + D = 104$ nm) and the internal diameter is D the volume of TiO$_2$ is:

$$V = \pi L (52^2 - (D/2)^2)$$

This relationship demonstrates that the amount of TiO$_2$ decreases as the inner diameter become more open. According to Choi et al. [25] the light depth penetration in a compact thin film of TiO$_2$ nanoparticles is limited to ~1.3 μm for wavelengths >300 nm.
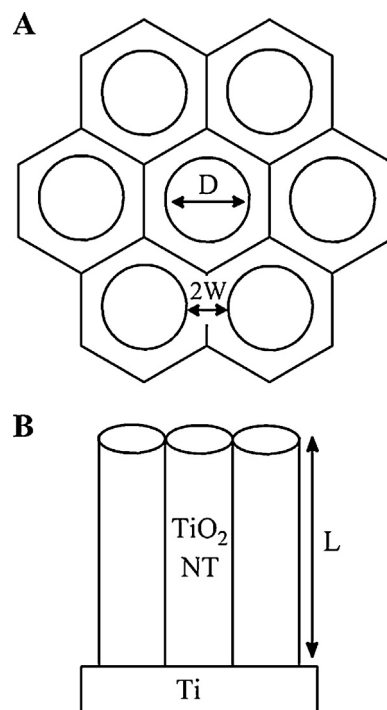
Scheme 2. Morphological features of TiO$_2$ nanotubes: (A) top-view and (B) side-view.

However the porosity of a nanotube array, is expected to be higher than a compact thin film of nanoparticles thus light should penetrate deeper in the tubes. Consequently we can assume that light is entirely absorbed in the first 1.5 μm region. Table 2 compares the volume of TiO$_2$ converting light into electron-hole pairs:

Based on Table 2, we can see that the amount of TiO$_2$ in the first 1.5 μm decreases as the tube length increases. Consequently light should be entirely absorbed on a longer distance. If we assume that light is entirely absorbed in the first 1,5 μm, 9.9 × 10^6 nm^3 of TiO$_2$ are required. For longer tubes, for example 13 μm (5.5 × 10^6 nm^3), for a same amount of TiO$_2$, light should be absorbed on almost 3 μm.
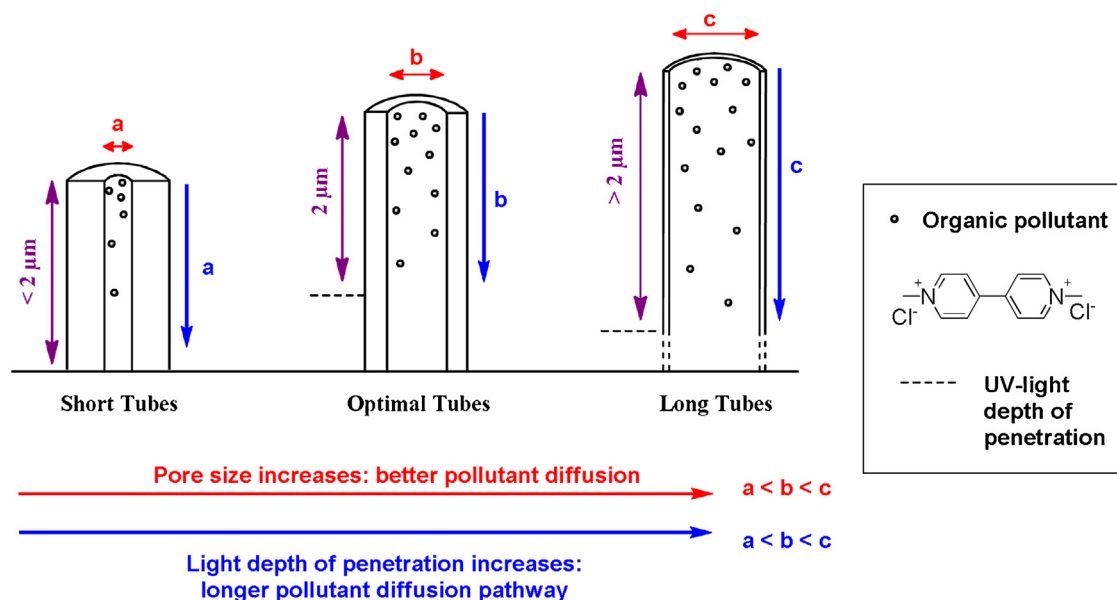
Scheme 3. Interpretation of the optimal photocatalytic activity for various top tube morphologies: short tubes (left), optimal tubes (center) and long tubes (right).

Table 1
Values of tube length with the corresponding average wall thickness and pore size (evaluated with SEM top-view).

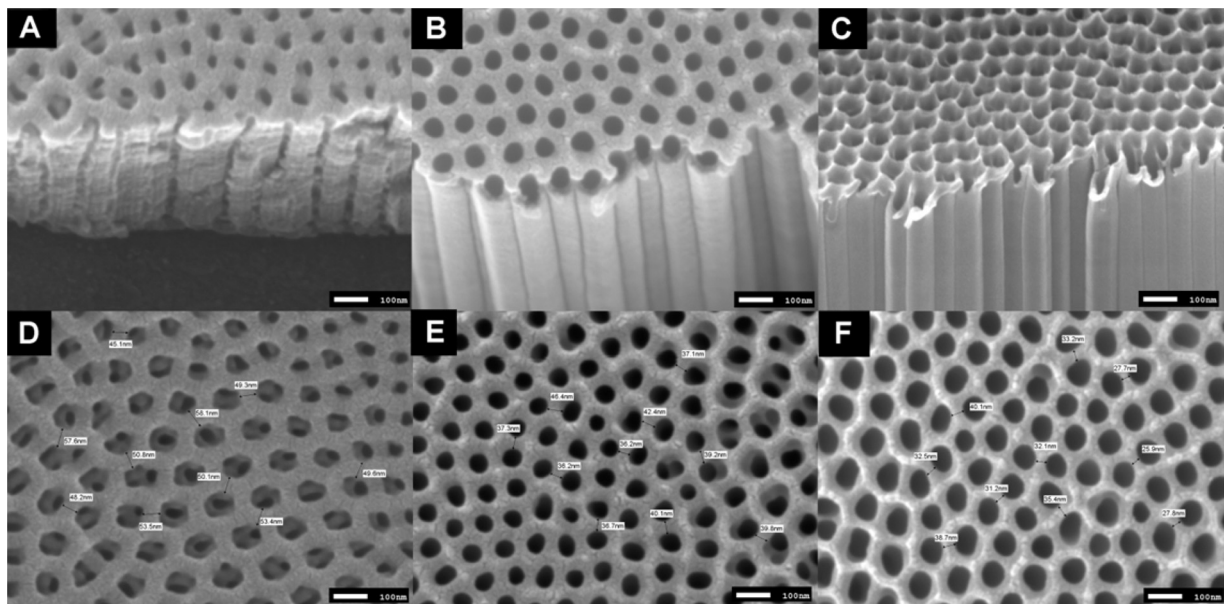| Sample ID	Anodization time (min)	Tube Length L (μm)	Wall thickness W (nm)	Internal diameter D (nm)
NT-1	5	1.5	27.7	49
NT-2	15	4.5	23.4	57
NT-3	30	7	19.5	64
NT-4	45	10	16.2	72
NT-5	50	13	13.4	78
NT-6	120	25	10.3	85

Fig. 1. SEM analysis – Side and Top view for various tube length: 1.5 μm (A, D), 7 μm (B, E) and 10 μm (C, F).

Table 2
Volume of TiO$_2$ for various samples in the first 1.5 μm.

Sample ID	Tube length L (μm)	Volume of TiO$_2$ V (nm^3)
NT-1	1.5	9.9×10^6
NT-2	4.5	8.9×10^6
NT-3	7	7.9×10^7
NT-4	10	6.6×10^6
NT-5	13	5.5×10^6
NT-6	25	4.2×10^6

Consequently electron-hole pairs would be generated further and the pollutant would travel a longer distance (diffusion controlled).

Fig. 2 shows the XRD pattern of a sample. The crystallization of TiO2 nanotubes at 450 °C allows to obtain a high anatase content. No rutile peaks were found. The anatase phase shows better photocatalytic properties due to higher electron mobility in the lattice of anatase compared to rutile [26].

Fig. 2. XRD diffractogram for TiO2 nanotubes.

3.2. Photocatalytic efficiencies

The photocatalytic activity of the TiO2 nanotubes was evaluated with the degradation of Paraquat. The concentration was followed by UV–vis spectroscopy. The nanotubes were first immersed in the Paraquat solution in the dark during 30 min to reach the adsorption equilibrium. Then the light was turned on (t = 0 min) and the photocatalytic degradation occurred. As we can see on Fig. 3, the photocatalytic degradation was followed by UV–vis spectroscopy at 257 nm corresponding to the maximum absorption peak of paraquat.

As we can see it on Fig. 3, paraquat's removal is followed by an increase of the absorption in the region 200–235 nm due to the

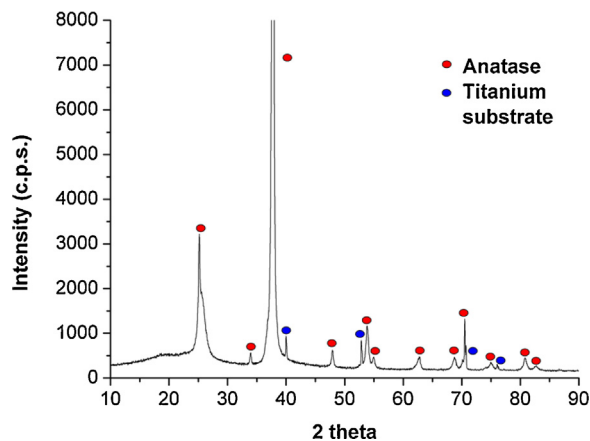formation of secondary products. For sufficiently long periods of degradation, the secondary products are not observed anymore.

Fig. 4 is a compilation of different degradation kinetics of paraquat for various tube lengths. We can see that the optimum is for 7 μm long tubes in our conditions. Moreover, short tubes (4.5 and 7 μm) have a better photocatalytic activity than other tubes.

These degradations follow a pseudo-first order law:

$$\ln(C/C_0) = -k \times t$$

where C is the concentration (0 for initial), k the kinetic constant (s^{-1}) and the time t. Consequently we obtain the following graph (fig. 5):
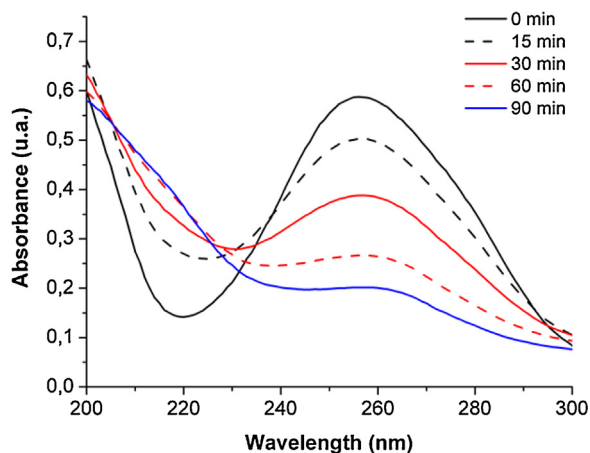
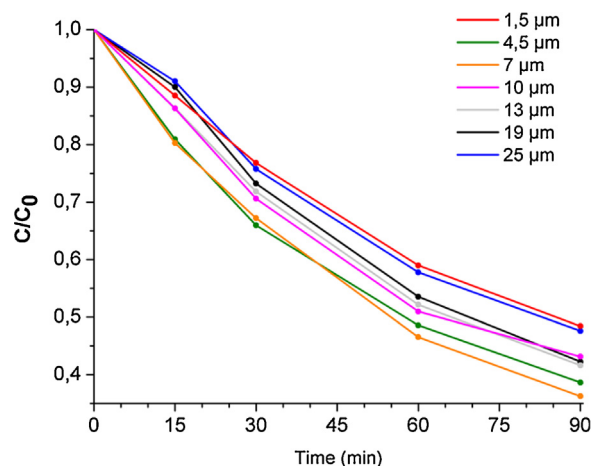**Fig. 3.** Photocatalytic degradation of paraquat followed by UV–vis spectroscopy.

Fig. 4. Degradation of Paraquat for various tube lengths.

Fig. 5 shows an optimum for tubes around 5–7 μm of length. This optimum should be correlated to the top tube morphology. Indeed the top-tube morphology presents a well defined open-mouth with relatively thick walls. This morphology is expected to exhibit a better photocatalytic activity as confirmed by Mazzarolo et al. [24]. According to the literature many different values were reported but the experimental conditions of growth are always different (concentration, temperature, applied potential). Consequently we believe that the presence of a well-defined open mouth depends on the synthetic conditions and the search of the optimum should be accurately determined. We developed a relatively simple model to rationalize the optimal photocatalytic activity (Scheme 3). When the tubes are short, the wall thickness is large thus the amount of TiO2 is important in the first micrometers. Consequently under illumination many electron-hole pairs are created. However the tube length must be sufficiently long to allow the entire UV light to be absorbed. On the other hand short tubes exhibit a relatively small inner diameter hindering pollutant diffusion (limiting step). When the tubes are longer, the light is entirely absorbed and the pollutant is degraded. When the tubes are longer than 7 μm, in our case, we observed a decrease in the photocatalytic activity. We believe that the volume of TiO_2 in the walls is decreasing thus light is absorbed on a longer pathway. Consequently, the pollutant should diffuse on a longer distance and the photocatalytic removal is controlled by diffusion.

In conclusion we attribute the optimal photocatalytic activity to a compromise between light absorption (thick walls absorb light on

a shorter distance, pollutant has to travel a short distance) and easy-access inside the tubes (large internal diameter improves pollutant diffusion). This interpretation is presented in Scheme 3.

This interpretation explains why different optimal photocatalytic activities were reported in the literature (6 μm, 16 μm, 17 μm and 18 μm). Indeed depending on the synthetic route, the well-defined open-mouth appears for different lengths. Consequently the variation of parameters such as pH, composition of the electrolyte, applied potential or temperature should strongly affect the optimal tube length for photocatalytic degradation of organic compounds.

4. Conclusion

The photocatalytic activity of TiO_2 nanotubes arrays strongly depends on the anodisation time. Short tubes with a small internal diameter exhibit poor photocatalytic activity because pollutant diffusion is ineffective. Long tubes have thin walls thus light is absorbed on a longer distance and pollutant has to diffuse further to reach the oxidizing species produced by the electron-hole pairs. The optimal tube length is given by a compromise between these two phenomenons.

Acknowledgements
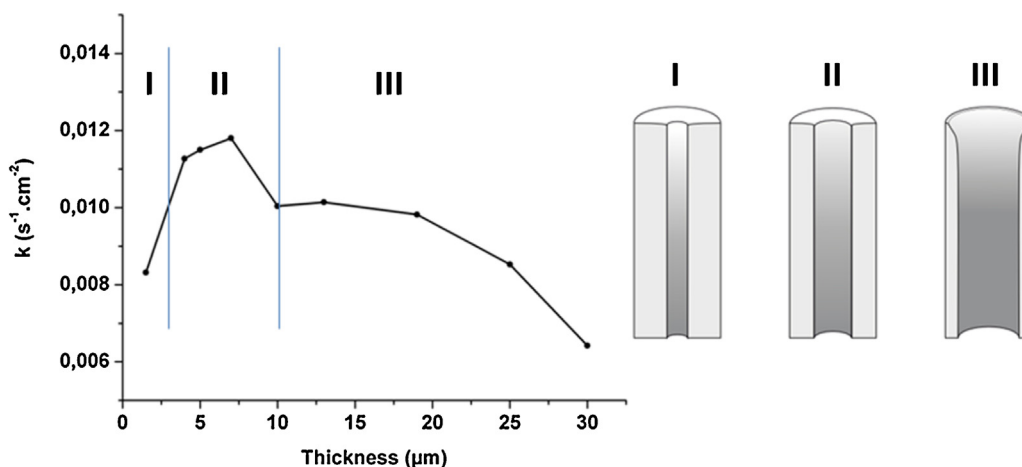
Fig. 5. Correlation between tube length and kinetic constant.

References

[1] F. a. P.C. Gobas, X. Zhang, R. Wells, Gastrointestinal magnification: the mechanism of biomagnification and food chain accumulation of organic chemicals, Environ. Sci. Technol. 27 (1993) 2855–2863, http://dx.doi.org/10.1021/es00049a028.

[2] M.N. Chong, B. Jin, C.W.K. Chow, C. Saint, Recent developments in photocatalytic water treatment technology: a review, Water Res. 44 (2010) 2997–3027, http://dx.doi.org/10.1016/j.watres.2010.02.039.

[3] P. Drogui, R. Daghrir, CO_2 sequestration, Biofuels Depollut. (2015), http://dx.doi.org/10.1007/978-3-319-11906-9.

[4] P. Roy, S. Berger, P. Schmuki, TiO2 nanotubes: synthesis and applications, Angew. Chem. Int. Ed. 50 (2011) 2904–2939, http://dx.doi.org/10.1002/anie.201001374.

[5] J. Lee, M. Kim, B. Kim, Removal of paraquat dissolved in a photoreactor with TiO 2 immobilized on the glass-tubes of UV lamps, Water Res. 36 (2002) 1776–1782.

[6] Q. Wang, X. Yang, X. Wang, M. Huang, J. Hou, Synthesis of N-doped TiO 2 mesosponge by solvothermal transformation of anodic TiO 2 nanotubes and enhanced photoelectrochemical performance, Electrochim. Acta 62 (2012) 158–162, http://dx.doi.org/10.1016/j.electacta.2011.12.009.

[7] E. Moctezuma, E. Leyva, E. Monreal, N. Viuegas, D. Infante, S.L. Potosf, et al., Photocatalytic degradation of the herbicide Paraquat, Chemosphere 39 (1999) 511–517.

[8] M. Kang, Preparation of TiO 2 photocatalyst film and its catalytic dichloride decomposition, Appl. Catal. B: Environ. 37 (2002) 187–196.

[9] M.J. Cantavenera, I. Catanzaro, V. Loddo, L. Palmisano, G. Sciandrello, Photocatalytic degradation of paraquat and genotoxicity of its intermediate products, J. Photochem. Photobiol. A: Chem. 185 (2007) 277–282, http://dx.doi.org/10.1016/j.jphotochem.2006.06.021.

[10] Z. Liu, Z. Jin, X. Liu, Y. Fu, G. Liu, Fabrication of ordered TiO2 porous thin films by sol-dipping PS template method, J. Sol-Gel Sci. Technol. 38 (2006) 73–78, http://dx.doi.org/10.1007/s10971-006-5035-0.

[11] S.J. Bu, Z.G. Jin, X.X. Liu, L.R. Yang, Z.J. Cheng, Synthesis of TiO2 porous thin films by polyethylene glycol templating and chemistry of the process, J. Eur. Ceram. Soc. 25 (2005) 673–679, http://dx.doi.org/10.1016/j.jeurceramsoc.2003.12.025.

[12] Z. Miao, D. Xu, J. Ouyang, G. Guo, X. Zhao, Y. Tang, Electrochemically induced sol-Gel preparation of single-Crystalline TiO2 nanowires, Nano Lett. 2 (2002) 717–720, http://dx.doi.org/10.1021/nl025541w.

[13] I. Paramasivam, H. Jha, N. Liu, P. Schmuki, A review of photocatalysis using self-organized TiO 2 nanotubes and other ordered oxide nanostructures, Small 8 (2012) 3073–3103, http://dx.doi.org/10.1002/smll.201200564.

[14] K. Lee, D. Kim, P. Roy, I. Paramasivam, B.I. Birajdar, E. Spiecker, et al., Anodic formation of thick anatase TiO 2 mesosponge layers for high efficiency photocatalysis, Mater. Sci. 7 (2010) 1–10.

[15] D. Kim, K. Lee, P. Roy, B.I. Birajdar, E. Spiecker, P. Schmuki, Formation of a non-thickness-limited titanium dioxide mesosponge and its use in dye-sensitized solar cells, Angew. Chem. Int. Ed. 48 (2009) 9326–9329, http://dx.doi.org/10.1002/anie.200904455.

[16] K. Lee, D. Kim, P. Schmuki, Highly self-ordered nanochannel TiO2 structures by anodization in a hot glycerol electrolyte, Chem. Commun. 47 (2011) 5789–5791, http://dx.doi.org/10.1039/c1cc11160d (Cambridge England).

[17] R. Daghrir, P. Drogui, D. Robert, Photoelectrocatalytic technologies for environmental applications, J. Photochem. Photobiol. A: Chem. 238 (2012) 41–52, http://dx.doi.org/10.1016/j.jphotochem.2012.04.009.

[18] K. Lee, A. Mazare, P. Schmuki, One-Dimensional titanium dioxide nanomaterials: nanotubes, Chem. Rev. (2014), http://dx.doi.org/10.1021/cr500061m.

[19] Y.R. Smith, A. Kar, V.R. Subramanian, Investigation of physicochemical parameters that influence photocatalytic degradation of methyl orange over TiO 2 nanotubes, Ind. Eng. Chem. Res. 48 (2009) 10268–10276.

[20] X. Zhang, K. Huo, L. Hu, Z. Wu, P.K. Chu, Synthesis and photocatalytic activity of highly ordered TiO2 and SrTiO3/TiO2 nanotube arrays on Ti substrates, J. Am. Ceram. Soc. 93 (2010) 2771–2778, http://dx.doi.org/10.1111/j.1551-2916.2010.03805.x.

[21] Z. Liu, X. Zhang, S. Nishimoto, M. Jin, D. a. Tryk, T. Murakami, et al., Highly ordered TiO 2 nanotube arrays with controllable length for photoelectrocatalytic degradation of phenol, J. Phys. Chem. C 112 (2008) 253–259, http://dx.doi.org/10.1021/jp0772732.

[22] C. Lin, Y. Yu, S. Chen, Y. Liou, Anodic growth of highly ordered titanium oxide nanotube arrays: effects of critical anodization factors on their photocatalytic activity, World Acad. Sci. Eng. Technol. (2010) 1094–1099.

[23] C. Das, P. Roy, M. Yang, H. Jha, P. Schmuki, Nb doped TiO(2) nanotubes for enhanced photoelectrochemical water-splitting, Nanoscale 3 (2011) 3094–3096, http://dx.doi.org/10.1039/c1nr10539f.

[24] A. Mazzarolo, K. Lee, A. Vicenzo, P. Schmuki, Anodic TiO2 nanotubes: influence of top morphology on their photocatalytic performance, Electrochem. Commun. 22 (2012) 162–165, http://dx.doi.org/10.1016/j.elecom.2012.05.037.

[25] W. Choi, S.J. Hong, Y.-S. Chang, Y. Cho, Photocatalytic degradation of polychlorinated dibenzo-p-dioxins on TiO 2 film under UV or solar light irradiation, Environ. Sci. Technol. 34 (2000) 4810–4815, http://dx.doi.org/10.1021/es0011461.

[26] T. Luttrell, S. Halpegamage, J. Tao, A. Kramer, E. Sutter, M. Batzill, Why is anatase a better photocatalyst than rutile?–Model studies on epitaxial TiO2 films, Sci. Rep. 4 (2014) 4043, http://dx.doi.org/10.1038/srep04043.